Astrophysical Journal

DRAFT VERSION AUGUST 11, 2006
Preprint typeset using LaTeX style emulateapj v. 26/01/00

AN UNUSUAL PRECURSOR BURST WITH OSCILLATIONS FROM SAX J1808.4–3658

SUDIP BHATTACHARYYA[1,2], AND TOD E. STROHMAYER[1]

Draft version August 11, 2006

ABSTRACT

We report the finding of an unusual, weak precursor to a thermonuclear X–ray burst from the accreting millisecond pulsar SAX J1808.4–3658. The burst in question was observed on Oct. 19, 2002 with the Rossi X-Ray Timing Explorer (RXTE) proportional counter array (PCA). The precursor began ≈ 1 s prior to the onset of a strong radius expansion burst, lasted for about 0.4 s, and exhibited strong oscillations at the 401 Hz spin frequency. Oscillations are not detected in the ≈ 0.5 s interval between the precursor and the main burst. The estimated peak photon flux and energy fluence of the precursor are about 1/25, and 1/500 that of the main burst, respectively. From joint spectral and temporal modeling, we find that an expanding burning region with a relatively low temperature on the spinning neutron star surface can explain the oscillations, as well as the faintness of the precursor with respect to the main part of the burst. We dicuss some of the implications of our findings for the ignition and spreading of thermonuclear flames on neutron stars.

Subject headings: methods: data analysis — stars: neutron — techniques: miscellaneous — X-rays: binaries — X-rays: bursts — X-rays: individual (SAX J1808.4–3658)

1. INTRODUCTION

Four strong thermonuclear (type-I) X–ray bursts were observed with *RXTE* proportional counter array (PCA) from the accreting millisecond pulsar SAX J1808.4–3658 when this source was in outburst in 2002 (Chakrabarty et al. 2003). Such bursts are produced by thermonuclear burning of matter accumulated on the surfaces of accreting neutron stars (Woosley, & Taam 1976; Lamb, & Lamb 1978). All the bursts exhibited strong brightness oscillations near the known stellar spin frequency (≈ 401 Hz; Wijnands & van der Klis 1998), which confirmed that this timing feature originates at the neutron star surface. During the burst rise, an expanding burning region (hot spot) on the spinning stellar surface may give rise to these oscillations (Strohmayer, Zhang & Swank 1997; Miller, & Lamb 1998; Nath, Strohmayer, & Swank 2002), while during the burst decay (when the whole stellar surface may be engulfed by thermonuclear flames), the origin of this timing feature may be temperature variations due to surface waves (Heyl 2005; Lee & Strohmayer 2005; Cumming 2005). Three of these bursts (Oct 15, 18 and 19) from SAX J1808.4–3658 exhibited strong oscillations during the intensity rise. Bhattacharyya & Strohmayer (2006c) found evidence for complex variation of the oscillation frequency during the rise of the Oct. 15 and 18 bursts. The Oct. 19 burst did not show evidence for similar variation, although the other properties of this burst were akin to those of the Oct. 15 and 18 bursts.

Analysis of high time resolution lightcurves just prior to the bursts reveal a weak precursor event to the Oct. 19 burst. To our knowledge this is the first report of such a precursor to a normal, hydrogen – helium powered thermonuclear burst. Several superbursts, which are likely powered by fusion of heavier elements (Strohmayer & Brown 2002; Cumming & Bildsten 2001; Schatz et al. 2002), have shown precursor events which have the characteristics of shorter, normal bursts. The precursor to the Oct. 19 burst looks like a typical thermonuclear burst except it lasts less than a second, and has a peak photon flux only 1/25 of the main burst. Also unique is the fact that strong pulsations are detected during this precursor. The Oct. 15 and 18 bursts do not show a similar precursor. In this Letter we describe the properties of the precursor, and discuss the implications for it's size and oscillation content in the context of ignition and spreading of thermonuclear instabilities on neutron stars.

2. DATA ANALYSIS, RESULTS AND SPECULATIONS

We analyzed the Oct. 19, 2002 archival *RXTE*-PCA data from SAX J1808.4–3658. During this observation the source was in outburst, and the data contain a thermonuclear X–ray burst, some of the properties of which were reported in Chakrabarty et al. (2003). We found an excess of intensity less than a second prior to the rise of this burst, that lasted for ≤ 0.5 s. Figure 1 shows the lightcurve of the burst at 1/16 s using a logarithmic intensity scale. The precursor is evident as the spike just prior to the rising edge of the main part of the burst. The precursor has a peak count rate of 2300 s^{-1} (1/16 s intervals, 4 PCUs), while the average persistent count rate prior to this feature was ~ 640 s^{-1}. This shows that the feature is significant. The rapid rise and slower decay of intensity during the precursor (see Fig. 2) is similar to that seen in most normal bursts, only the peak intensity and timescale are smaller and shorter, respectively. The spectra of thermonuclear bursts can usually be modelled with a blackbody function (Strohmayer & Bildsten 2006). We, therefore, fitted the precursor spectrum (using 0.25 s of data) with an absorbed blackbody and found a temper-

[1]X-ray Astrophysics Lab, Exploration of the Universe Division, NASA's Goddard Space Flight Center, Greenbelt, MD 20771; sudip@milkyway.gsfc.nasa.gov, stroh@clarence.gsfc.nasa.gov

[2]Department of Astronomy, University of Maryland at College Park, College Park, MD 20742-2421

ature of $1.26^{+0.10}_{-0.13}$ keV (reduced $\chi^2 \approx 1.4$, 28 degrees of freedom, see Figure 2). The reduced χ^2 is acceptable, and supports the idea that the precursor is indeed thermonuclear in origin.

Next, we searched for oscillations in the 0.3 s of event mode data (shown with dotted lines in Figure 2) for which the precursor intensity was significantly above the persistent level. We computed a power spectrum with a Nyquist frequency of 2048 Hz, and a frequency resolution of 3.3 Hz, and found a peak (power level ≈ 43.9) near the known stellar spin frequency ~ 401 Hz (Fig. 3). As burst oscillation frequencies are not known to evolve by more than ≈ 6 Hz (Giles et al. 2002; Muno et al. 2002; Bhattacharyya & Strohmayer 2005), considering the number of trials $N_{\rm trial} = 2$, we have a significance of 6.01×10^{-10}, which implies a $> 6\sigma$ detection of oscillations during the precursor. The fractional rms amplitude for this 0.3 s interval is $A_1 = 0.375 \pm 0.068$ (reduced $\chi^2 = 7.0/13$ from fitting a constant+sinusoid model to the persistent emission subtracted, phase-folded light curve), and no significant harmonic component was detected. This high amplitude and the comparatively broad peak in the power spectrum show that these oscillations originate from the precursor, and are not accretion-powered pulsations. We also calculated dynamic Z^2 power spectra (Strohmayer & Markwardt 1999). The corresponding power contours show that the oscillations during the precursor are unique to it, and, for example, the oscillations seen on the rising portion of the main burst are an additional phenomenon (see Figure 2).

Now, several important questions are: (1) why does the precursor occur about a second prior to the main burst, and (2) why was it so much fainter than the main burst. Note that this burst may not be considered as a single double-peaked non-photospheric radius expansion (non-PRE) burst, because such bursts are always weak (ie. sub-Eddington, Sztajno et al. 1985), while the main burst was a strong PRE burst. Therefore, sequential emissions from two different portions of the neutron star surface (Bhattacharyya & Strohmayer 2006a; 2006b), or a two step energy generation due to convective mixing of the nuclear fuel (Fujimoto et al. 1988) probably cannot explain the precursor event. A two step energy release might answer the first question. The second question may be addressed in the following way. Near the peak of the main burst, most of the neutron star surface is expected to emit near the Eddington temperature. Therefore, a smaller emission region and/or a lower temperature during the precursor would explain its faintness compared to the main burst. This might happen in three ways: (1) if the fuel for the precursor is confined to a small portion of the stellar surface (possibly by the magnetic field) and the burning region has a high temperature (the small hot spot can produce high amplitude, spin modulated pulsations); (2) if the thermonuclear flame spreads all over the stellar surface in < 0.1 s at the onset of the precursor, and the whole surface emits at a low temperature (in such a case, surface modes might account for the oscillations; see § 1); and (3) if the thermonuclear flame with an intermediate average temperature takes ~ 0.2 s to spread (in this case, the expanding hot spot may give rise to the oscillations). Joint timing and spectral modeling can help us discriminate between these alternatives.

To be more specific about the joint analysis, we first note that the ratio (*Ratio*) of the observed persistent emission subtracted photon flux near the peak of the main burst (the last time bin of the lower panel of Fig. 2; hereafter bin 1) to that during the precursor (the first bin of the lower panel of Fig. 2; hereafter bin 2) is 25.1 ± 1.5 (the energy flux ratio is about 45 to 1). The corresponding observed blackbody temperatures during these bins are $T_{\rm obs,1} = 2.94 \pm 0.13$ keV and $T_{\rm obs,2} = 1.26^{+0.10}_{-0.13}$ keV (mentioned before) respectively. We also note that the fractional rms amplitude of oscillations during bin 2 is $A_2 = 0.403 \pm 0.071$. From our spectral modeling we also find that the precursor contained only $\approx 1/400$ of the energy in the main burst. Now for the joint modeling, assuming the stellar and other source parameter values, one needs to reproduce the oscillation amplitude A_2, and then, with the same parameter values (including the average burning region size), one needs to reproduce *Ratio* from $T_{\rm obs,1}$ and $T_{\rm obs,2}$. We do this in § 3.2.

3. COMPARISON WITH MODELS

The primary aim of our modeling is to understand both the faintness of the precursor (relative to the peak of the burst), and the presence of high amplitude brightness oscillations. In our simple model, we assume emission from a circular burning region (hot spot) on the rotating stellar surface (Bhattacharyya et al. 2005). Brightness oscillations occur as the image of the hot spot in the observer's sky periodically changes with the stellar spin. The corresponding fractional rms amplitude (A) can be determined by fitting the phase-folded light curve (normalised to have the observed count rate). The total observed photon flux can also be computed from the blackbody spectrum for an assumed temperature. For these calculations, we combine the model with the appropriate instrument response matrix. Our model includes the following physical effects: (1) Doppler effect due to rapid stellar spin, (2) special relativistic beaming, and (3) gravitational redshift and light bending (assuming Schwarzschild spacetime). In our numerical calculations, we track the paths of photons in order to incorporate the light bending effect in the calculated photon flux (Bhattacharyya, Bhattacharya, & Thampan 2001). We use the following parameters in our model: (1) neutron star mass M (in $M_\odot$), (2) dimensionless stellar radius-to-mass ratio Rc^2/GM, (3) stellar spin frequency ν (≈ 401 Hz; § 1), (4) observer's inclination angle i measured from the upper rotational pole, (5) polar angle of the hot spot center $\theta_{\rm c}$, (6) angular radius of the hot spot $\Delta\theta$, and (7) the blackbody temperature $T_{\rm BB}$. For SAX J1808.4–3658, Li et al. (1999) and Bhattacharyya (2001) calculated constraints on M and Rc^2/GM (although they assumed that the stellar magnetic field is entirely dipolar). For example, if the lower limit of Rc^2/GM is 4.0, the upper limit of M is ~ 1.4 (equation 6 of Bhattacharyya 2001). Here for our illustrative model, we assume $M = 1.4$ and $Rc^2/GM = 4.0$. However, other values of M and Rc^2/GM in reasonable ranges do not alter our conclusions significantly. In our calculations, we mostly use $i = 60°$, as this is the average value for a randomly oriented stellar spin axis. We use $i \approx 80°$ as the upper limit, because the absence of a deep eclipse indicates $i < 82°$ (Chakrabarty & Morgan 1998). For a source distance $d = 3$ kpc, Wang et

al. (2001) suggested $i \approx 20^\circ - 65^\circ$ (with 90% confidence) based on the modeling of the X–ray and optical emission from SAX J1808.4–3658. A higher value of d (3.4 – 3.6 kpc; Galloway & Cumming 2006) would shift this range of i towards slightly smaller values. We, therefore, consider the case $i = 40^\circ$ in our joint spectral and timing modeling in § 3.2. We vary the other parameter values for our model calculations.

3.1. *Inferences from Timing Data*

Before conducting the joint spectral and timing modeling, we explore whether or not a hot spot model can reproduce the observed amplitude $A_1 = 0.375 \pm 0.068$ (§ 2) during the precursor. A burning region with $i = 60^\circ$, $\theta_c = 60^\circ$, $\Delta\theta = 60^\circ$ and the observed $T_{BB} = 1.26$ keV gives the amplitude $A = 0.364 \pm 0.048$, which is consistent with A_1. Here we note that the harmonic content of this model light curve cannot be significantly detected because of the small number of observed counts, consistent with the observations. Next, we change T_{BB} to = 1.0 keV, which does not alter A ($= 0.372 \pm 0.048$) much, and $i = 80^\circ$ can also reproduce A_1 for similar values of θ_c, $\Delta\theta$ and T_{BB}. We note that A increases with the increase of i and θ_c (up to $\theta_c = 90^\circ$), and with the decrease of $\Delta\theta$. For example, keeping $i = 60^\circ$ and $T_{BB} = 1.26$ keV, if we change θ_c to 45°, then to reproduce an A ($= 0.354 \pm 0.048$) which is consistent with A_1, $\Delta\theta$ has to be 5°. This demonstrates two points: (1) for fixed values of other parameters and a lower limit on $\Delta\theta$ (such a lower limit should exist, as the burning region has to have a finite size; Spitkovsky, Levin, & Ushomirsky 2002), there is a lower limit on θ_c; and (2) the size of the burning region cannot be meaningfully constrained from the lower side using the observed oscillation amplitude alone. However, this size can be constrained from the upper side, as $i = 80^\circ$ and $\theta_c = 90^\circ$ (that allow the near-maximum value of $\Delta\theta$ for a given oscillation amplitude A_1) gives $\Delta\theta_{max} \sim 90^\circ$. Therefore, our modeling of the timing data shows that a hot spot, that does *not* encompass most of the stellar surface, can give rise to the observed oscillation amplitude.

3.2. *Joint Spectral and Timing Inferences: An Illustration*

For our joint modeling (last paragraph of § 2), we assume emission from the whole stellar surface during bin 1 (a time bin during the peak of the main burst; see § 2). This is because a smaller burning region would give rise to significant oscillations (which are not observed at this time), and would probably imply a super-Eddington luminosity. For this analysis, we consider the same values of M, Rc^2/GM, ν and i (as mentioned earlier in this section), and vary the values of θ_c and $\Delta\theta$ for the precursor. However, for T_{BB}, we use the surface color temperature T_c, which is related to the observed temperature T_{obs} by $T_c = T_{obs}(1+z)$ (where the surface gravitational redshift $1 + z = (1 - 2GM/Rc^2)^{-1/2}$). Moreover, due to spectral hardening in the neutron star atmosphere, the effective surface temperature (T_{eff}) is related to T_c by $T_{eff} = T_c/f$, where the color factor f is greater than 1 (London, Taam, & Howard 1984). Therefore, in order to calculate the observed photon flux, we use $(1/f^4)B(E_{em}, T_c)$ as the emitted specific intensity (Fu & Taam 1990; Bhattacharyya et al. 2001). Here, B is the Planck function and E_{em} is the energy of a photon in the emitter's frame. Özel (2006) has recently suggested the following expression for f (based on the model atmosphere calculations of Madej, Joss, & Różańska 2004): $f = 1.34 + 0.25((1 + X)/1.7)^{2.2}((T_{eff}/10^7\mathrm{K})^4/(g/10^{13}\mathrm{cm/s^2}))^{2.2}$. Here, the surface gravitational acceleration g is given by $(GM/R^2)(1 - 2GM/Rc^2)^{-1/2}$, and X is the hydrogen mass fraction. For our illustrative model, initially we assume the cosmic abundance $X = 0.7$ for both bin 1 and bin 2 (time bins from Fig. 2; see the last paragraph of § 2). However, we note that a change in the value of X does not alter our timing results, as the oscillation amplitude does not depend on f, and hence on X. For our assumed values of the parameters, $f = 1.805$ ($T_{eff,1} = 2.30$ keV; bin 1) and 1.344 ($T_{eff,2} = 1.33$ keV; bin 2). Here we note that, although $T_{eff,1}$ is high, the corresponding luminosity is less than (but close to) the Eddington luminosity, which shows the consistency among our assumed parameter values.

Now, we follow the procedure that is described in the last paragraph of § 2. First, we calculate the photon flux (for $f = 1.805$) for the emission from the whole stellar surface at the color temperature $T_c = 4.16$ keV (corresponding to $T_{obs,1}$; bin 1). Then we compute the oscillation amplitude A and the photon flux for bin 2 using $T_{BB} = 1.78$ keV (i.e., T_c corresponding to $T_{obs,2}$), $f = 1.344$, and various values of i, θ_c and $\Delta\theta$. For $i = 60^\circ$, $\theta_c = 65^\circ$ and $\Delta\theta = 55^\circ$, we find $A = 0.398 \pm 0.050$ and *Ratio* = 25.3, which are consistent with A_2 and the observed value of *Ratio* respectively. These two observed parameter values can also be reproduced for $i = 80^\circ$ for slightly different values of θ_c and $\Delta\theta$. Moreover, for $i = 40^\circ$, $\theta_c = 110^\circ$ and $\Delta\theta = 67^\circ$, we get $A = 0.391 \pm 0.050$ and *Ratio* = 25.7. These show that our simple hot spot model is consistent with the timing and the spectral data simultaneously, and the inferred size of the hot spot (i.e., burning region) is similar to that inferred in § 3.1. For $i = 60^\circ$, $\theta_c = 50^\circ$, and $\Delta\theta = 5^\circ$, A ($= 0.378 \pm 0.050$) is consistent with A_2, but *Ratio* (= 2504.3) is widely different from the observed value. This shows that the spectral data do not allow a small hot spot for the precursor burst. In fact, for a variable θ_c and for $i = 60^\circ$ (and other assumed parameter values), $\Delta\theta$ cannot be much less than 55°. As in § 3.1, we next try to determine $\Delta\theta_{max}$ for $i = 80^\circ$ and $\theta_c = 90^\circ$. We can reproduce A_2 well for $\Delta\theta = 85^\circ$, but the corresponding *Ratio* (= 13.8) is much less than the observed value. Therefore, spectral data indicate that $\Delta\theta < 85^\circ$, and support the inference from the timing data (§ 3.1), that the average angular radius of the burning region of the precursor cannot be much larger than 90°.

In the previous paragraph, we assumed $X = 0.7$ for both the time bins. But if the precursor (bin 2) and the main burst (bin 1) were ignited at different layers of accreted matter (§ 2), X_{prec} might be greater than X_{main}. Here we assume the extreme values ($X_{prec} = 0.7$, i.e., hydrogen-rich, and $X_{main} = 0.0$, i.e., helium-rich), and check if the inferences of the previous paragraph still hold. Clearly, the new value of X_{main} alters (increases) only the photon flux for bin 1 (as f becomes 1.654), and hence the value of *Ratio* changes. For $i = 60^\circ$, $\theta_c = 75^\circ$ and $\Delta\theta = 70^\circ$ (for bin 2), we find $A = 0.389 \pm 0.050$ and *Ratio* = 25.3, which are consistent with the observed values. Therefore,

our simple hot spot model can simultaneously explain both the timing and the spectral data, even when the chemical composition of the burning matter of the two bursts are very different. For $X_{\rm main} = 0.0$, as the value of f (for bin 1) decreases, and hence the corresponding model photon flux increases, the model photon flux (and hence the hot spot size) of the precursor has to increase in order to reproduce the observed *Ratio*. Therefore, a small hot spot is even more disfavored for $X_{\rm prec} = 0.7$ and $X_{\rm main} = 0.0$. But do these extreme values of X allow a precursor burning region that is much larger than 90°? For $i = 80°$ and $\theta_{\rm c} = 90°$ (for bin 2), we can reproduce A_2 for $\Delta\theta = 85°$, but the corresponding *Ratio* (= 19.7) is significantly less than the observed value. Therefore, even when the chemical composition of the bursts are considerably different, the modeling of the spectral data indicate $\Delta\theta \lesssim 90°$ for the precursor.

The results of our modeling show that the burning region during the precursor burst was neither small, nor large enough to cover most of the stellar surface. This argues againts scenarios 1 and 2 for the faintness of the precursor compared to the main burst (see § 2). Therefore, it is likely that during the precursor the burning region (with a relatively low temperature) expanded for ~ 0.2 s, and $\Delta\theta$ of our model represents an average angular radius during time bin 2. The expanding burning region can naturally account for the observed oscillations, and when the burning covered most of the stellar surface, the oscillations ceased.

4. DISCUSSION AND CONCLUSIONS

In this Letter, we have reported the discovery of a unique precursor to a thermonuclear burst that; (1) occured about a second prior to the main burst, (2) existed for a portion of a second, (3) had a peak intensity more than a order of magnitude less than that of the main peak, and (4) showed strong spin modulation pulsations. With relatively simple modeling, we have found that an expanding burning region at a relatively low temperature can explain the oscillations, as well as the faintness of the precursor.

The low temperature and fluence of the precursor (compared to the main peak) suggests that the amount of fuel involved in the precursor is small compared to the total available for the whole burst. It would seem that there are at least three possibilities to account for the precursor. In the first scenario the release of nuclear energy at depth could have such a two-step time dependence. In this case the observed time dependence would be a direct reflection of the time dependent energy release due to nuclear burning. In the second class of models, the precursor could be produced by a physical separation of fuel layers. This, combined with the finite energy transport time-scale through the surface layers results in the observed two-step energy release. This scenario, or one very like it, is thought to be responsible for the precursors observed with superbursts (see Strohmayer & Brown 2002; Strohmayer & Markwardt 2003). In superbursts, ignition is thought to occur via unstable carbon burning, perhaps in a background of heavy *rp*-process ashes (Cumming & Bildsten 2001; Schatz et al. 2001; Strohmayer & Brown 2002). This occurs at much greater column depths ($\approx 2 \times 10^{12}$ g cm^{-2}) than the unstable helium burning which ignites normal bursts ($\approx 2 \times 10^{8}$ g cm^{-2}; Woosley et al. 2004). The energy released at depth by a superburst diffuses upwards and, partially, inwards. The outward going flux triggers the hydrogen - helium fuel above it, resulting in the precursor burst. In this case, the combination of radial separation of the fuel layers and finite energy diffusion time-scales results in the observed precursor.

A third possibility is that the precursor acts as a "trigger" which initiates the burst. If unstable burning begins somewhere on the star at a column depth above that where simple considerations of the ignition physics would suggest then it could act as a "spark," setting off the remaining combustible fuel below. To date, most theoretical investigations have considered ignition conditions based on spherically symmetric perturbations. Recent observations, in the context of burst oscillations, suggest that non-axisymmetric processes are likely crucial for a complete understanding of ignition and spreading. Recent theoretical work has also reached this conclusion (see Spitkovsky, Levin & Ushomirsky 2002). Perhaps temperature, composition, and or accretion gradients across the stellar surface might bring about such a condition. Once nuclear energy release begins locally, then heat will flow from that layer both in and out. If ignition conditions are relatively finely "balanced," then it might not take much additional heat flux to set off the rest of the fuel. While the physical quantities which govern ignition are almost certainly not uniform across the star, it remains uncertain whether such conditions vary enough to make this kind of triggering possible.

Can we say whether either of these alternatives is at work (or not) in the October 19, 2000 burst? Based on the recent study of Galloway & Cumming (2006) it seems highly likely that the bursts from SAX J1808.4–3658 were ignited in a helium rich environment. While the exact nuclear composition is not known, and indeed, details of some of the relevant nuclear processes are uncertain, it seems unlikely, though not impossible, that a pure helium ignition would have such a delayed energy release. For example, the calculations of Woosley et al. (2004) indicate a rapid, monotonic rise of the luminosity from helium-rich ignitions, although we note that these were one-dimensional (radial) calculations. We suggest it is more likely that a situation like the 2nd or 3rd scenarios is responsible for the precursor, but it is difficult to be more precise with only the one example at present.

An additional clue might be the fact that the Oct. 19 burst was the last observed (of the 4 bursts detected), and happened at the lowest accretion rate (see Galloway & Cumming 2006). Previous theoretical work has shown that there exists an accretion rate regime in which bursts can be triggered by unstable hydrogen burning (Fujimoto Hanawa & Miyaji 1981; Fushiki & Lamb 1987; Narayan & Heyl 2003). Galloway & Cumming (2006) argue that the bursts observed from SAX J1808.4–3658 in October 2002 were in or near the pure helium shell ignition regime, with the accretion rate per unit area of the stellar surface $\dot{m} \sim 1{,}000$ g cm^{-2} s^{-1}. This is close to the critical $\dot{m}$ below which stable hydrogen burning switches off (see, for example, Fujimoto et al. 1981). If $\dot{m}$ dropped below this threshold some time after the 3rd burst, then an accumulating hydrogen layer could form above a partially formed

helium layer. If unstable burning were then triggered in the hydrogen layer, it would inject enough energy to raise the temperature and stabilize the hydrogen burning, but it might not take much additional energy input to destabilize the helium layer below, and set off the remainder of the accreted fuel. This could explain the faintness of the precursor in that the burning timescale is longer for the temperature-dependent CNO cycle (than for the triple-α process), and/or the fact that it might only take a small amount of energy to stabilize the hydrogen burning once started (Fujimoto et al. 1981) . We speculate that such a process might explain the precursor.

If this reasoning is correct then the duration of the precursor, t_{dur}, and the time between it's start and the rising edge of the main burst, $\Delta t_{pre} \approx 1$ s, can provide some rough constraints on several relevant time-scales. If energy must flow inward to trigger the main burst, and then flow back out–for us to see the main burst–then Δt_{pre} is approximately twice the radiative diffusion time from the trigger layer to the column depth of helium fuel responsible for the main burst. This gives a diffusion time-scale of ≈ 0.5 s, which is roughly consistent with theoretical calculations (Cumming & Bildsten 2000). While we do not claim to be able to precisely infer this quantity, the fact that it is in qualitative agreement with theoretical expectations provides some support for the idea of radially separated fuel layers.

What about spreading time-scales? For this scenario to work the intensity profile of the precursor would have to be largely controlled by the spreading of the hydrogen burning layer. In order to account for the overall rise-time and duration of the precursor, the spreading time would have to be approximately several tenths of seconds. Indeed, the rise and decay of the precursor would directly represent lateral spreading across the surface. This time-scale would also accomodate the observed duration of the oscillations during the precursor. One would likely require that the cooling time for the hydrogen layer be less than or of order the spreading time, or else the decay of the precursor would be difficult to understand. We note that there is evidence for weak emission between the precursor and main burst (see Figure 1), which provides some support for the idea that the initial (possibly hydrogen) energy release had a longer time-scale. Finally, we reported evidence that this burst had a somewhat different frequency evolution of the oscillations observed on the rising edge (of the main burst) compared to the two other bursts (Bhattacharyya & Strohmayer 2006c). It may be possible that the different ignition condition suggested here also contributed to this difference.

While the arguments above seem to provide a reasonable qualitative description, they will remain largely speculative until more detailed calculations are done. It is another indication that high quality data is forcing us to explore interesting details of nuclear burning on neutron stars. Indeed it seems clear that these results point towards the necessity of a realistic, three dimensional model of thermonuclear ignition and flame spreading that considers all the major physical effects including magnetic field, stellar spin, chemical composition, and time variable accretion.

REFERENCES

Bhattacharyya, S. 2001, ApJ, 554, L185
Bhattacharyya, S., Bhattacharya, D., & Thampan, A. V. 2001, MNRAS, 325, 989
Bhattacharyya, S., & Strohmayer, T. E. 2005, ApJ, 634, L157
Bhattacharyya, S., & Strohmayer, T. E. 2006a, ApJ, 636, L121
Bhattacharyya, S., & Strohmayer, T. E. 2006b, ApJ, 641, L53
Bhattacharyya, S., & Strohmayer, T. E. 2006c, ApJ, 642, L161
Bhattacharyya, S., Strohmayer, T. E., Miller, M. C., & Markwardt, C. B. 2005, ApJ, 619, 483
Chakrabarty, D. et al. 2003, Nature, 368, 42
Chakrabarty, D., & Morgan, E. H. 1998, Nature, 394, 346
Cumming, A. 2005, ApJ, 630, 441
Cumming, A. & Bildsten, L. 2000, ApJ, 544, 453
Fu, A., & Taam, R. E. 1990, ApJ, 353, 205
Fujimoto, M. Y., Hanawa, T. & Miyaji, S. 1981, ApJ, 246, 267
Fujimoto, M. Y., Sztajno, M., Lewin, W. H. G., & van Paradijs, J. 1988, A&A, 199, L9
Galloway, D. K., & Cumming, A. 2006, ApJ, in press (astro-ph/0607213)
Giles, A. B., Hill, K. M., Strohmayer, T. E., & Cummings, N. 2002, ApJ, 568, 279
Heyl, J. S. 2005, MNRAS, 361, 504
Lamb, D. Q., & Lamb, F. K. 1978, ApJ, 220, 291
Lee, U., & Strohmayer, T. E. 2005, MNRAS, 361, 659
Li, X.-D., Bombaci, I., Dey, M., Dey, J., & van den Heuvel, E. P. J. 1999, Phys. Rev. Lett., 83, 3776
London, R. A., Taam, R. E., & Howard, W. M. 1984, ApJ, 287, L27
Madej, J., Joss, P. C., & Różańska, A. 2004, ApJ, 602, 904
Miller, M. C. & Lamb, F. K. 1998, ApJ, 499, L37
Muno, M. P., Chakrabarty, D., Galloway, D. K., & Psaltis, D. 2002, ApJ, 580, 1048
Nath, N. R., Strohmayer, T. E. & Swank, J. H. 2002, ApJ, 564, 353
Özel, F. 2006, Nature, in press (astro-ph/0605106)
Schatz, H. et al. 2001, Phys. Rev. Lett., 86, 16, 3471
Spitkovsky, A., Levin, Y. & Ushomirsky, G. 2002, ApJ, 566, 1018
Strohmayer, T. E., & Bildsten, L. 2006, in *Compact Stellar X-ray Sources*, Eds. W.H.G. Lewin and M. van der Klis, (Cambridge University Press: Cambridge), (astro-ph/0301544)
Strohmayer, T. E. & Brown, E. F. 2002, ApJ, 566, 1045
Strohmayer, T. E., & Markwardt, C. B. 1999, ApJ, 516, L81
Strohmayer, T. E., Zhang, W. & Swank, J. H. 1997, ApJ,
Sztajno, M. et al. 1985, ApJ, 299, 487
Wang, Z. et al. 2001, ApJ, 563, L61
Wijnands, R., & van der Klis, M. 1998, Nature, 394, 344
Woosley, S. E. et al. 2004, ApJS, 151, 75
Woosley, S. E., & Taam, R. E. 1976, Nature, 263, 101

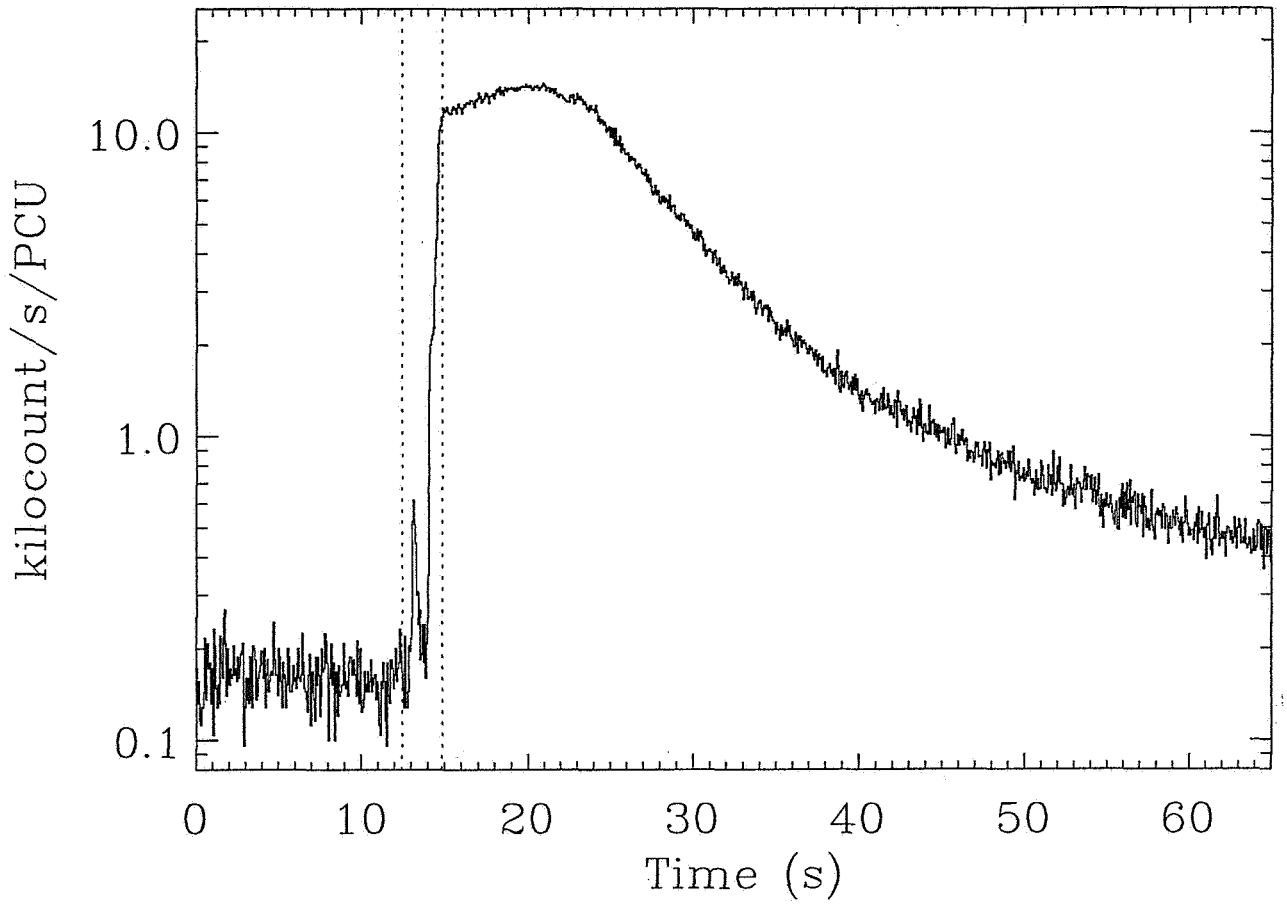

FIG. 1.— A thermonuclear X–ray burst in the Oct. 19, 2002 *RXTE* PCA data from the accreting millisecond pulsar SAX J1808.4–3658. The burst shows a clear precursor event. The dotted vertical lines give the time interval that is shown in Fig. 2. Note that the vertical scale is logarithmic.

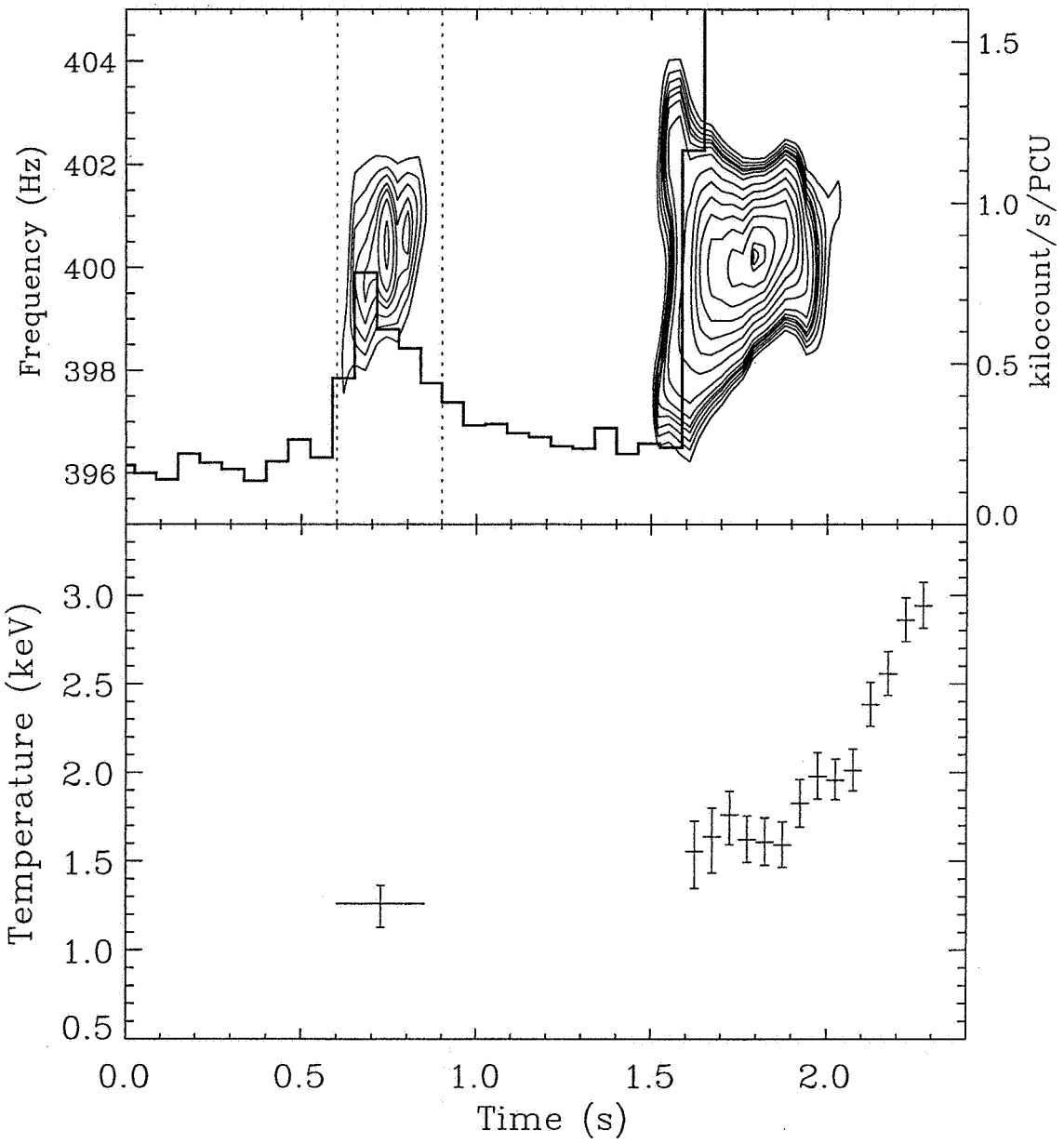

FIG. 2.— Intensity and temperature profiles of the Oct. 19 burst. The upper panel gives the detected intensity and the power contours (minimum and maximum power values are 30 and 50 for the precursor, and 30 and 122.9 for the main burst) from the dynamic power spectra (for 0.3 s duration at 0.03 s intervals). The dotted vertical lines give the time interval for which a power spectrum has been shown in Fig. 3. The lower panel shows the blackbody temperatures inferred from the model fitting of the time resolved burst spectra (persistent emission subtracted and deadtime correction applied). Here the horizontal lines give the binsize and the vertical lines give the 90% confidence intervals.

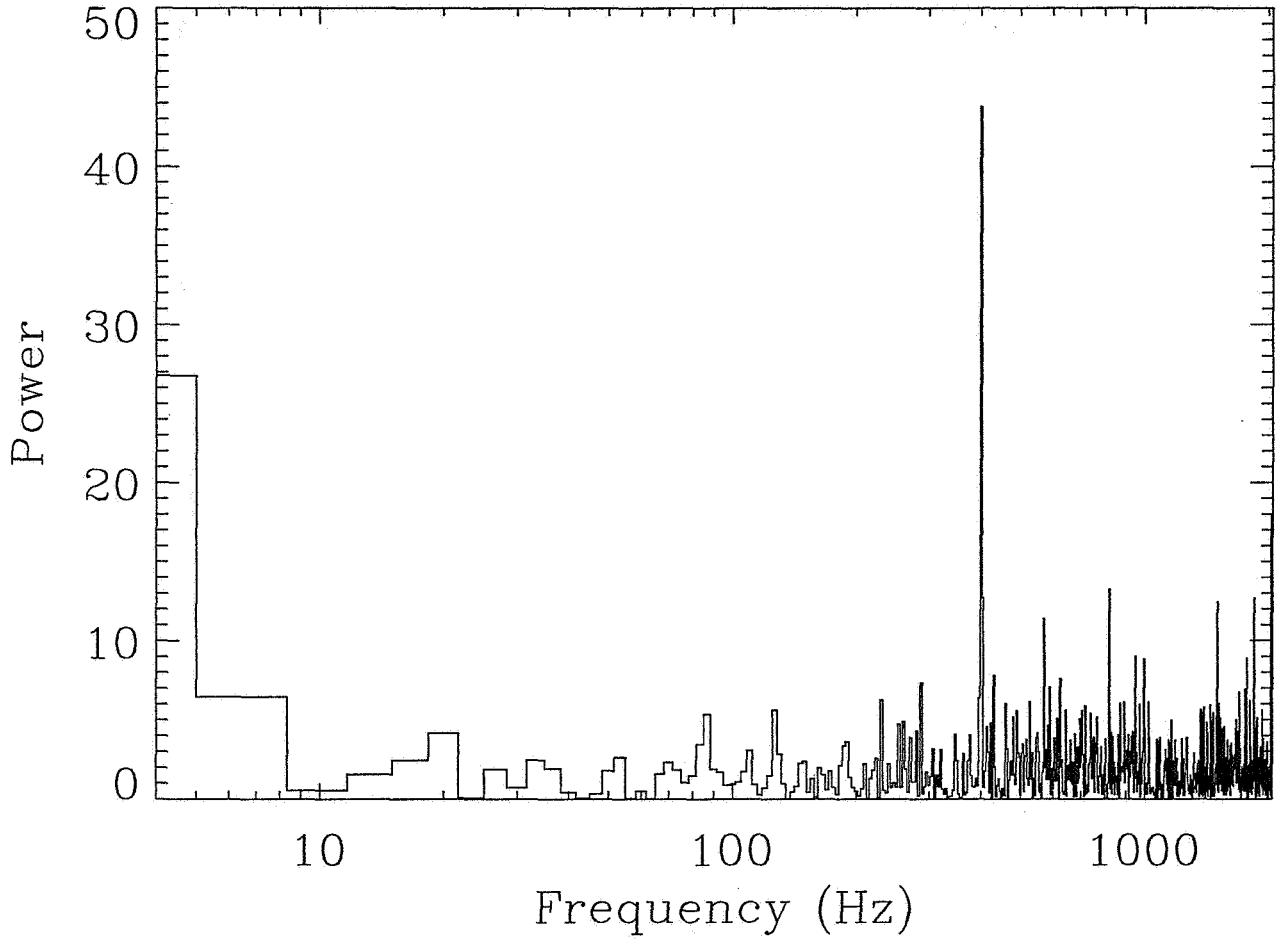

FIG. 3.— Power spectrum for 0.3 s time interval during the short-lived precursor burst from (see Fig. 2). The peak near 400 Hz indicates strong burst oscillations.